sure within the PIPAAm-modified capillary at 30 °C and burst release during PIPAAm collapse. This burst is analogous to drug release from collapsing PIPAAm gel disks undergoing analogous thermal treatment.[17] Similarly, just after each temperature return to 30 °C, small fluores-cent spikes are observed. In contrast, oscillatory fluorescent changes have been observed using 0.5 min cyclic intervals (shown in Fig. 3c) indicating subtle PIPAAm swell–shrink transition kinetics affecting flow profiles. Aqueous flow has been blocked completely using air bubbles in PIPAAm-grafted capillaries ($\varphi = 200$ μm) above the PIPAAm transition temperature, where the microchannel surfaces are hydrophobic, trapping the air bubble.[30] Our microfluidic channels distinguish their flow-control behavior by completely blocking water flow via PIPAAm graft hydration. Considerably higher pressure is required to initiate water flow through PIPAAm-grafted capillaries below PIPAAm's collapse-transition temperature. Thermally regulated flow control in PIPAAm-grafted capillaries is rapid and reversible, facilitating many reliable and repeated open–close cycles. Such reversible, thermally modulated, polymer-grafted on–off switches for controlling microfluidic behavior might be regulated locally on-chip using optical signals (local infrared heating), resistive heating microelements, or external thermostats. Spatial control is possible using patterned grafted capillaries and different polymer-grafted areas with chemistries exhibiting distinct phase-transition behavior in designated locations. Opportunities for new microvalve systems exploiting this basic design are substantial.

Received: December 20, 2004
Final version: July 13, 2005
Published online: September 22, 2005

[1] A. Hatch, A. E. Kamholz, K. R. Hawkins, M. S. Munson, E. A. Schilling, B. H. Weigl, P. Yager, *Nat. Biotechnol.* **2001**, *19*, 461.
[2] O. Hofmann, G. Voirin, P. Niedermann, A. Manz, *Anal. Chem.* **2002**, *74*, 5243.
[3] R. K. Marcus, W. C. Davis, B. C. Knippel, L. LaMotte, T. A. Hill, D. Perahia, J. D. Jenkins, *J. Chromatogr., A* **2003**, *986*, 17.
[4] M. Tokeshi, T. Minagawa, K. Uchiyama, A. Hibara, K. Sato, H. Hisamoto, T. Kitamori, *Anal. Chem.* **2002**, *74*, 1565.
[5] J. W. Hong, S. R. Quake, *Nat. Biotechnol.* **2003**, *21*, 1179.
[6] S. Takayama, J. C. McDonald, E. Ostuni, M. N. Liang, P. J. A. Kenis, R. F. Ismagilov, G. M. Whitesides, *Proc. Natl. Acad. Sci. USA* **1999**, *96*, 5545.
[7] A. Wolff, I. R. Perch-Nielsen, U. D. Larsen, P. Friis, G. Goranovic, C. R. Poulsen, J. P. Kutter, P. Telleman, *Lab Chip* **2003**, *3*, 22.
[8] M. U. Kopp, A. J. de Mello, A. Manz, *Science* **1998**, *280*, 1046.
[9] B. H. Weigl, P. Yager, *Science* **1999**, *283*, 346.
[10] S. Lee, W. Jeong, D. J. Beebe, *Lab Chip* **2003**, *3*, 164.
[11] D. J. Beebe, J. S. Moore, J. M. Bauser, Q. Yu, R. H. Liu, C. Devadoss, B. H. Jo, *Nature* **2000**, *404*, 588.
[12] E. C. Peters, F. Svec, J. M. J. Fréchet, *Adv. Mater.* **1997**, *9*, 630.
[13] C. Yu, S. Mutlu, P. Selvaganapathy, C. H. Mastrangelo, F. Svec, J. J. Fréchet, *Anal. Chem.* **2003**, *75*, 1958.
[14] Q. Luo, S. Mutlu, Y. B. Gianchandani, F. Svec, J. M. J. Fréchet, *Electrophoresis* **2003**, *24*, 3694.
[15] D. Huh, A. H. Tkaczyk, J. H. Bahng, Y. Chang, H. H. Wei, J. B. Grotberg, C. J. Kim, K. Kurabayashi, S. Takayama, *J. Am. Chem. Soc.* **2003**, *125*, 14 678.
[16] S. Z. Hua, F. Sachs, D. X. Yang, H. D. Chopra, *Anal. Chem.* **2002**, *74*, 6392.
[17] R. Yoshida, K. Sakai, T. Okano, Y. Sakurai, Y. H. Bae, S. W. Kim, *J. Biomater. Sci., Polym. Ed.* **1991**, *3*, 155.
[18] M. Matsukata, T. Aoki, K. Sanui, N. Ogata, A. Kikuchi, Y. Sakurai, T. Okano, *Bioconjugate Chem.* **1996**, *7*, 96.
[19] N. Yamada, T. Okano, H. Sakai, F. Karikusa, Y. Sawasaki, Y. Sakurai, *Makromol. Chem., Rapid Commun.* **1990**, *11*, 571.
[20] M. Yamato, T. Okano, *Mater. Today* **2004**, *7*, 42.
[21] T. Shimizu, M. Yamato, Y. Isoi, T. Akutsu, T. Setomaru, K. Abe, A. Kikuchi, M. Umezu, T. Okano, *Circ. Res.* **2002**, *90*, E40.
[22] K. Nishida, M. Yamato, Y. Hayashida, K. Watanabe, N. Maeda, H. Watanabe, K. Yamamoto, S. Nagai, A. Kikuchi, Y. Tano, T. Okano, *Transplantation* **2004**, *77*, 379.
[23] A. Kikuchi, T. Okano, *Prog. Polym. Sci., Jpn.* **2002**, *27*, 1165.
[24] H. Kanazawa, K. Yamamoto, Y. Matsushima, N. Takai, A. Kikuchi, Y. Sakurai, T. Okano, *Anal. Chem.* **1996**, *68*, 100.
[25] J. Kobayashi, A. Kikuchi, K. Sakai, T. Okano, *Anal. Chem.* **2003**, *73*, 2027.
[26] M. Heskins, J. E. Guillet, E. James, *J. Macromol. Sci., Chem.* **1968**, *2*, 1441.
[27] T. Norisuye, N. Masui, Y. Kida, D. Ikuta, E. Kokufuta, S. Ito, S. Panyukov, M. Shibayama, *Polymer* **2002**, *43*, 5289.
[28] R. Yoshida, K. Uchida, Y. Kaneko, K. Sakai, A. Kikuchi, Y. Sakurai, T. Okano, *Nature* **1995**, *374*, 240.
[29] Y. Akiyama, A. Kikuchi, M. Yamato, T. Okano, *Langmuir* **2004**, *20*, 5506.
[30] T. Saitoh, Y. Suzuki, M. Hiraide, *Anal. Sci.* **2002**, *18*, 203.

Synthesis and Electronic Properties of Individual Single-Walled Carbon Nanotube/Polypyrrole Composite Nanocables**

By *Xiaolei Liu*, *James Ly*, *Song Han*, *Daihua Zhang*, *Ari Requicha*, *Mark E. Thompson*, and *Chongwu Zhou**

Synthesizing composite materials is an effective way to combine the features of different materials and tailor the properties to achieve the desired material performance. Carbon fiber composite research can be traced back to the 1950s and was targeted at improving the mechanical properties of

[*] Prof. C. Zhou, X. Liu, S. Han, D. Zhang
Department of Electrical Engineering—Electrophysics
University of Southern California
Los Angeles, CA 90089 (USA)
E-mail: chongwuz@usc.edu
J. Ly, Prof. M. E. Thompson
Department of Chemistry, University of Southern California
Los Angeles, CA 90089 (USA)
Prof. A. Requicha
Department of Computer Science, University of Southern California
Los Angeles, CA 90089 (USA)

[**] We gratefully acknowledge support from a NSF CAREER Award, a NSF-CENS grant, a SRC/MARCO Award, a NSF-NIRT grant (CCR-01-20778), and the DARPA MolApps Program (SPAWAR SysCtr San Diego, #N66001-04-1-8902).

 DOI: 10.1002/adma.200501211

ADVANCED MATERIALS

materials, due to the needs of the space and aircraft industries for strong, lightweight structural materials.[1] Compared with traditional carbon fibers, carbon nanotubes (CNTs) possess unique electronic structures and extraordinary electrical, optical, chemical, and mechanical properties.[2] For instance, single-walled carbon nanotubes (SWCNTs) have a very long mean free path on the order of a micrometer, ultrahigh carrier mobility up to 79 000 $cm^2 V^{-1} s^{-1}$,[3] high current sustainability beyond 10^9 $A cm^{-2}$,[4] and can be either metallic or semiconducting with different bandgaps depending on the nanotube chirality and diameter.[5] Based on these important properties, ballistic conducting channels[6] and field-effect transistors[7] have been demonstrated with individual carbon nanotubes. In addition, SWCNTs are very sensitive to the environment due to their high surface-to-volume ratios, which make them acute chemical and biological sensors.[8–11] In parallel with the advances in the nanotube field, polypyrrole (PPy) has emerged as an important conducting polymer, and has been used in a wide range of applications,[12–16] including artificial muscles[17] and chemical sensing.[18–22] Significant efforts have been devoted to the research on CNT/polymer composites, for example, with the goal of enhancing the polymer conductivity for light-emitting and photovoltaic applications.[23–26] These composite materials have also been demonstrated to exhibit improved sensing reproducibility and device yield.[27] These studies, however, have been limited to bulk nanotube/PPy composites usually consisting of large amounts of entangled nanotube bundles within a PPy film; these composites are complicated systems with significant intertube hopping for the charge carriers.

In this paper, we present our work on the synthesis, transport studies, and chemical sensing applications of individual SWCNT/PPy nanocables, which represent a unique and highly ordered SWCNT/polymer composite. This is achieved by first patterning source/drain electrodes to individual SWCNTs grown on a Si/SiO_2 substrate (using chemical vapor deposition, CVD), and then coating the nanotube with PPy by electrochemical deposition. Surprisingly, these devices exhibited suppressed conductance after the initial conducting PPy deposition for both metallic and semiconducting nanotubes, in sharp contrast to the anticipated combined conductance from both the nanotubes and PPy coating. In addition, further deposition of PPy led to an eventual recovery in conductance, which is attributed to the increased conductance of the PPy layer due to increased thickness. Furthermore, these composite materials have been demonstrated to work as chemical sensors, with enhanced conductance upon NO_2 exposure and reduced conductance upon NH_3 exposure. Our work reveals the rich and intriguing properties of nanotube/PPy composites beyond previous studies on bulk systems.

We started with the fabrication of individual SWCNT devices using CVD and photolithography.[28] In brief, catalyst islands were deposited onto Si/SiO_2 substrates, and then CVD was carried out to produce single-walled carbon nanotubes with diameters of ~1–3 nm. Metal contacts with a separation of 3 μm were subsequently deposited to contact individual carbon nanotubes. The PPy coating was then electrochemically deposited onto the SWCNT with doubly distilled pyrrole as the feedstock and sodium tetrafluoroborate as the electrolyte. After polymerization, the sample was lightly rinsed with deionized water and dried with nitrogen. This has consistently led to PPy deposited over both the carbon nanotubes and the source/drain electrodes. Figure 1a shows a schematic of a synthesized SWCNT/PPy nanocable, where PPy is depicted as a half-cylinder covering the nanotube. Figure 1b shows an

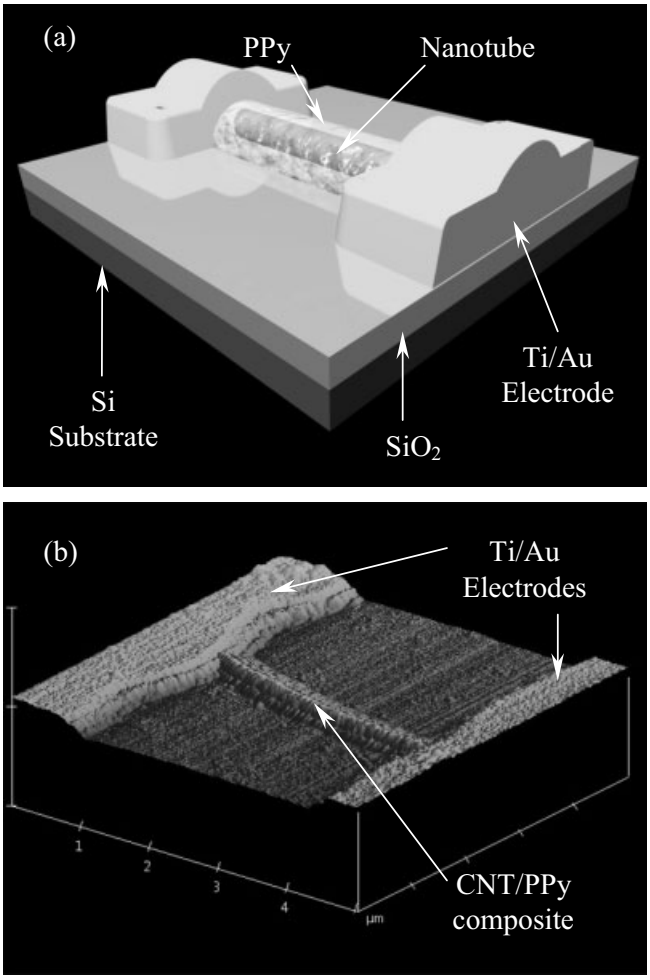

Figure 1. a) Schematic of an individual SWCNT/PPy composite nanocable device. b) Atomic force microscopy (AFM) image of a SWCNT/PPy nanocable.

atomic force microscopy (AFM) image of a typical SWCNT device with PPy deposited for 60 min, where an individual nanotube bridging the source/drain electrodes can be clearly seen with a PPy coating. Careful examination of the AFM images before and after the PPy deposition reveals a PPy coating ~60 nm in thickness, which appeared grainy but nevertheless continuous. No deposition of PPy has been observed over the insulating SiO_2 substrates. A study of the time dependence of

the PPy film growth on SWCNTs was carried out. We started with a bare carbon nanotube device, carried out the PPy deposition for 5 min, and then used AFM to determine the height of the nanotube/PPy nanocable. The sample was returned to the electrochemical cell for further PPy deposition, and the height subsequently recorded using AFM. This process was repeated several times until a nanocable height of 127 nm was reached. Figure 2a displays the data points of the nanocable height versus the deposition time; this plot can be fitted with a linear deposition rate of ~1 nm min^{-1}.

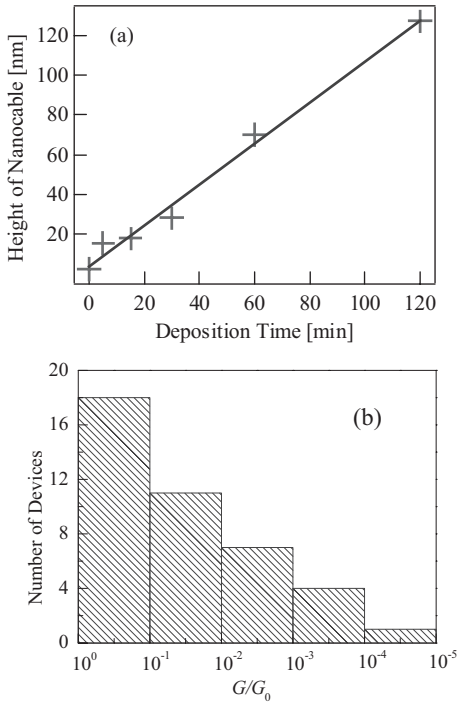

Figure 2. a) Plot of the SWCNT/PPy height versus the deposition time. b) Histogram showing number of devices versus G/G_0 (G_0 and G are the device conductance before and after PPy deposition, respectively).

These CNT/PPy composite nanocable devices provide ideal systems to study the effect of the PPy coating on the carbon nanotubes, as individual nanocables with metallic contacts can be easily produced. This eliminates the complicated carrier transport path associated with bulk nanotube/PPy composites, and therefore enables in-depth studies on these devices. We have measured the conductance of a batch of 30 devices before and after the deposition of 60 nm of PPy. Figure 2b displays a histogram of the number of devices versus G/G_0, where G_0 and G are the device conductance before and after the PPy deposition, respectively. All the devices exhibited suppressed conductance after the PPy deposition by a factor of $2 \sim 10^4$. We repeated the same procedure for several batches of devices and all the devices displayed similar behavior.

To study the details of this conductance suppression, we chose devices with an individual SWCNT connecting the electrodes for further studies, including both metallic and semiconducting nanotube devices. Figure 3 depicts the behavior of a typical device with a metallic CNT between the electrodes. Figure 3a displays a scanning electron microscopy (SEM) image of the device before the PPy coating, showing one nanotube bridging the electrodes. Figure 3b shows an SEM image of the same device after the PPy coating. One can clearly see the PPy coating around the nanotube and the electrodes, and more importantly, the nanotube remained intact after the PPy coating. As shown in Figure 3c inset, this device displayed little gate dependence before the PPy deposition, thus confirming the nanotube was metallic. The curves in Figure 3c correspond to the current–voltage (I–V) curves of the device before and after the PPy deposition, as indicated. Detailed analysis of these curves revealed zero-bias conductance values of 21.4 μS and 7.3 μS for before and after PPy deposition, respectively, indicating conductance suppression by a factor of three. In comparison to metallic nanotube devices, Figure 4 displays results from a device with a typical p-type semiconducting nanotube connecting source and drain electrodes before the PPy coating. Figures 4a and b display the SEM images of the device before and after the 60 nm PPy coating, respectively, showing only one nanotube bridging the source/drain electrodes and no noticeable damage to the nanotube after the PPy deposition. The I–V curves in Figure 4c were taken with the gate voltage $V_g = -20$ V on samples before and after the PPy deposition, as indicated. The linear conductance is derived to be 0.93 μS for curve of the sample before PPy deposition and 1.58 nS for the curve of the sample after PPy deposition, corresponding to conductance suppression by a factor of 590. Figure 4d shows the I–V_g curve taken with the drain–source voltage $V = 50$ mV before the PPy deposition. Typical p-type nanotube transistor behavior was observed, as the conductance decreased monotonically to almost zero when the gate voltage was swept from –10 V to 10 V. In con-

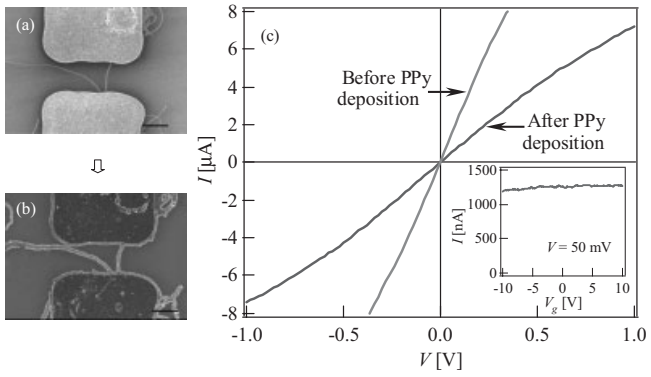

Figure 3. Scanning electron microscopy images of a metallic nanotube device a) before and b) after 60 nm PPy deposition. The scale bars represent 2 μm. c) Current–voltage (I–V) curves of the device before and after the PPy coating, showing suppressed conduction. Inset: I–V_g (V_g: gate voltage) curve of the device before PPy coating, showing metallic behavior.

ADVANCED MATERIALS

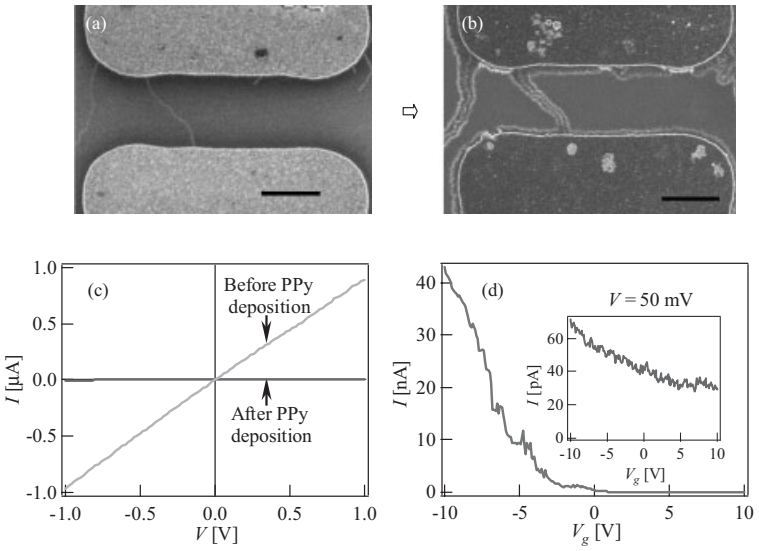

Figure 4. SEM images of a semiconducting nanotube device a) before and b) after 60 nm PPy deposition. The scale bars represent 2 μm. c) *I–V* curves of the device before and after the PPy coating ($V_g = -20$ V). d) *I–V*$_g$ curve of the device before PPy coating. Inset: *I–V*$_g$ curve of the device after PPy coating.

trast, the *I–V*$_g$ curve taken with the same device after the coating of 60 nm PPy displayed much lower current values (70–30 pA) and relatively weak p-type semiconductor behavior.

The conductance suppression for carbon nanotube devices with 60 nm PPy coating is therefore convincingly established for both metallic and semiconducting nanotubes. The details of the interaction between the nanotube and the deposited polymer was rarely studied in previous publications on bulk composite materials,[23–26] and intuitively one would simplify the electronic properties of the SWCNT/polymer nanocable to two parallel connected conduction channels made of the nanotube and the polymer coating. Our results clearly show that the nanotube/PPy composite systems are more complicated than the simplified parallel conduction channel model. The observed conductance suppression in our nanotube/PPy nanocables may originate from several factors. The first is the formation of scattering centers close to the nanotube when PPy was deposited. PPy coating is known to incorporate various ions, which could work as coulombic scattering centers for carriers in the carbon nanotube. Enhanced carrier scattering may lead to conductance suppression for both metallic and semiconducting nanotubes. We further suggest that the deposited PPy might form covalent bonds with the nanotube at the defect sites and subsequently lead to enhanced scattering. Even though the nanotube sidewall is very inert and resistant to chemical bonding with the PPy during the electrochemical deposition, the dangling bonds at defect sites can be highly reactive and ready for covalent bonding with the deposited PPy. Confirmation of the covalent bonding, however, is difficult due to the low density of defects associated with nanotubes grown via CVD. An additional relevant factor is the change of contact resistance when both the metal electrodes and the nanotubes are coated with PPy. For semiconducting nanotube transistors, it is well known that the device resistance consists of contribution from both the contacts and the bulk nanotube.[29] The PPy coating may significantly alter the Schottky barrier at the metal–nanotube contacts and contribute to the observed conductance suppression. We note that the nanotube/polymer composites represent complicated systems due to their nanoscale dimensions and the involvement of defects and contacts. Further in-depth studies are needed to fully elucidate the nanotube/polymer interaction, which could lead to tailor-made functional materials. We have also examined the effect of PPy of different thicknesses on the electronic properties of the composite nanocables. Interestingly, we have consistently observed the suppression of conductance upon initial PPy deposition and the eventual recovery of conductance when the PPy thickness approaches 100 nm (see Supporting Information). We attribute the conductance recovery to the increased conduction through the PPy coating layer, which becomes increasingly important as more PPy is deposited onto the nanotube.

In addition to the transport studies, we have further studied the sensing properties of our CNT/PPy composite nanocables and demonstrated gas sensors responsive to both oxidizing and reducing gases such as NO_2 and NH_3. Our devices have a major advantage over traditional film sensors due to their high surface-to-volume ratio. In these experiments, the as-made CNT/PPy devices were bonded and transferred into an airtight chamber, stabilized in an argon environment, and then exposed to a gas flow of either NO_2 or NH_3 diluted in argon. Figure 5a displays *I–V* curves recorded in argon, 100 ppm NO_2, and 1000 ppm NO_2, showing an increase in conductance at higher NO_2 concentration. In contrast, Figure 5c shows the sensing response of a different device to NH_3 of various concentrations, and a monotonic reduction in conduction at higher NH_3 concentration can be clearly seen. This behavior indicates that the nanotube/PPy composite is a p-type semiconductor, as enhanced conductance was observed upon exposure to an oxidizing gas (i.e., NO_2), and suppressed conductance was observed for exposure to a reducing gas (i.e., NH_3). Figures 5b,d are plots of the device conductance versus the NO_2 and NH_3 concentration, respectively. The solid lines represent fits using the Langmuir adsorption model, which is suitable for gas adsorption on non-microporous surfaces.[30,31] We noticed that the response of our devices saturated at high concentrations of NH_3, but no obvious saturation was observed for NO_2 within the concentration range available to us. This may stem from the fact that NO_2 has much higher binding efficiency on PPy than NH_3, and thus the response did not saturate even for 1000 ppm NO_2. The results here clearly show the potential of the nanotube/PPy composite for chemi-

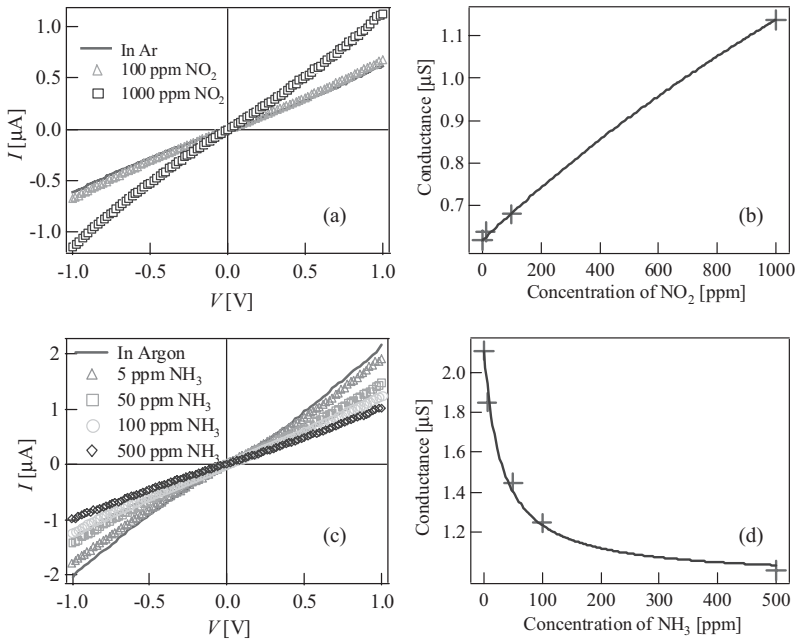

Figure 5. *I–V* curves of SWCNT/PPy nanocable devices exposed to a) NO_2 and c) NH_3 of different concentrations. b,d) Plots of the device conductance vs. NO_2 and NH_3 concentrations, respectively. Solid lines are fitted curves based on the Langmuir isotherm adsorption model.

cal sensing applications, though we note that the sensitivity achieved so far is lower than that of bare carbon nanotube devices.[8]

In summary, we have developed a novel way to synthesize individual SWCNT/PPy composite nanocables based on nanotube field-effect transistors. These devices exhibited surprising suppressed conductance for thin and moderate PPy coatings (~60 nm) for both metallic and semiconducting nanotubes. The amplitude of the suppression varies from device to device and falls within a broad range of 2–10^4 times that of the CNT conductance before PPy deposition. In addition, a recovery in conductance was observed with nanotube/PPy nanocables upon further deposition of PPy, which is attributed to the conduction through the conducting PPy layer. Furthermore, these composite materials have been demonstrated to work as chemical sensors, with enhanced conductance upon NO_2 exposure and reduced conductance upon NH_3 exposure. Our work clearly illustrates that nanotube/polymer composite systems are more complicated than the simplified parallel-conduction-channel model would suggest. The interaction between the nanotubes and the polymer coating deserves further in-depth studies and may provide challenges as well as opportunities for practical applications.

Experimental

Carbon nanotube devices were prepared using a CVD technique. First, a Si substrate covered with a 500 nm thick SiO_2 layer was chosen, and deep UV lithography was used to open the windows at the sites of the catalyst. Then a mixture of $Fe(NO_3)_3$ and Al_2O_3 powder in methanol was dispersed on the substrate. After liftoff of the unwanted catalyst, the substrate was loaded into a tube furnace (Lindberg/Blue Mountain) and heated up to 900 °C under a mixed gas flow of H_2, C_2H_4, and CH_4 in the ratio 1:60:200. After 10 min of growth, the substrate was allowed to cool down to room temperature followed by photolithography to define the metal electrodes. Finally, 3 nm Ti capped with 60 nm Au was deposited to form the source and drain contacts to the nanotubes.

PPy was electrochemically deposited onto the SWCNT using a single-cell compartment consisting of an aqueous solution of 0.1 M pyrrole (Aldrich), which was doubly distilled, and 0.2 M sodium tetrafluoroborate (Aldrich). Gold bonding wires connecting the nanotube devices comprised the working electrode, while a glassy carbon rod (Alfa Aesar) served as the counter electrode, and Ag/AgCl (Corning) served as the reference electrode. The electrochemical formation of PPy was carried out at a constant voltage of 0.5 V (versus Ag/AgCl) at room temperature using a potentiostat (Princeton Applied Research 283). The thickness of the PPy coating was controlled by tuning the deposition time.

The as-made nanotube devices were examined by SEM (Hitachi 4800 operated at 1 keV) and AFM (DI NanoScope III in tapping mode). All electrical measurements were carried on a probe station (Wentworth Labs) using a semiconductor parameter analyzer (Agilent 4156B).

Received: June 13, 2005
Final version: August 11, 2005
Published online: September 29, 2005

[1] R. Bacon, *J. Appl. Phys.* **1960**, *31*, 283.
[2] M. S. Dresselhaus, G. Dresselhaus, P. Avouris, *Carbon Nanotubes: Synthesis, Structure, Properties and Applications*, Springer-Verlag, Berlin **2001**.
[3] T. Durkop, S. A. Getty, E. Cobas, M. S. Fuhrer, *Nano Lett.* **2004**, *4*, 35.
[4] Z. Yao, C. L. Kane, C. Dekker, *Phys. Rev. Lett.* **2000**, *84*, 2941.
[5] R. Saito, M. Fujita, G. Dresselhaus, M. S. Dresselhaus, *Appl. Phys. Lett.* **1992**, *80*, 2204.

ADVANCED MATERIALS

[6] W. Liang, M. Bockrath, D. Bozovic, J. H. Hafner, M. Tinkham, H. Park, *Nature* **2001**, *411*, 665.
[7] A. Javey, J. Guo, Q. Wang, M. Lundstrom, H. Dai, *Nature* **2003**, *424*, 654.
[8] J. Kong, N. R. Franklin, C. Zhou, M. G. Chapline, S. Peng, K. Cho, H. Dai, *Science* **2000**, *287*, 622.
[9] P. G. Collins, K. Bradley, M. Ishigami, A. Zettle, *Science* **2000**, *287*, 1801.
[10] R. J. Chen, S. Bangsaruntip, K. A. Drouvalakis, N. W. S. Kam, M. Shim, Y. M. Li, W. Kim, P. J. Utz, H. J. Dai, *Proc. Natl. Acad. Sci. USA* **2003**, *100*, 4984.
[11] A. Star, J. C. P. Gabriel, K. Bradley, G. Gruner, *Nano Lett.* **2003**, *3*, 459.
[12] O. Patil, A. J. Heeger, F. Wudl, *Chem. Rev.* **1988**, *88*, 183.
[13] P. Novak, K. Muller, K. S. V. Santhanam, O. Haas, *Chem. Rev.* **1997**, *97*, 207.
[14] K. Haupt, K. Mosbach, *Chem. Rev.* **2000**, *100*, 2495.
[15] E. Coronado, C. J. Gomez-Garcia, *Chem. Rev.* **1998**, *98*, 273.
[16] K. Tajima, T. Aida, *Chem. Commun.* **2000**, 2399.
[17] M. Trojanowicz, *Microchim. Acta* **2003**, *143*, 75.
[18] R. H. Baughman, *Synth. Met.* **1996**, *78*, 339.
[19] B. J. Hwang, J.-Y. Yang, C.-W. Lin, *J. Electrochem. Soc.* **1999**, *146*, 1231.
[20] F. Yue, T. S. Ngin, G. Hailin, *Sens. Actuators, B* **1996**, *32*, 33.
[21] D. T. McQuade, A. E. Pullen, T. M. Swager, *Chem. Rev.* **2000**, *100*, 2537.
[22] K. J. Albert, N. S. Lewis, C. L. Schauer, G. A. Sotzing, S. E. Stitzel, T. P. Vaid, D. R. Walt, *Chem. Rev.* **2000**, *100*, 2595.
[23] S. A. Curran, P. M. Ajayan, W. J. Blau, D. L. Carroll, J. N. Coleman, A. B. Dalton, A. P. Davey, A. Drury, B. McCarthy, S. Maier, A. Strevens, *Adv. Mater.* **1998**, *10*, 1091.
[24] J.-Y. Kim, M. Kim, J.-H. Choi, *Synth. Met.* **2003**, *139*, 565.
[25] H. Ago, K. Petritsch, M. S. P. Shaffer, A. H. Windle, R. H. Friend, *Adv. Mater.* **1999**, *11*, 1281.
[26] E. Kymakis, I. Alexandrou, G. A. J. Amaratunga, *J. Appl. Phys.* **2003**, *93*, 1764.
[27] K. H. An, S. Y. Jeong, H. R. Hwang, Y. H. Lee, *Adv. Mater.* **2004**, *16*, 1005.
[28] J. Kong, H. T. Soh, A. M. Cassell, C. F. Quate, H. J. Dai, *Nature* **1998**, *395*, 878.
[29] J. Appenzeller, J. Knoch, V. Derycke, R. Martel, S. Wind, P. Avouris, *Phys. Rev. Lett.* **2002**, *89*, 126 801.
[30] P. Qi, O. Vermesh, M. Grecu, A. Javey, Q. Wang, H. Dai, *Nano Lett.* **2003**, *3*, 347.
[31] D. Zhang, Z. Liu, C. Li, T. Tang, X. Liu, S. Han, B. Lei, C. Zhou, *Nano Lett.* **2004**, *4*, 1919.

Selective Construction of Supramolecular Nanotube Hosts with Cationic Inner Surfaces

By *Naohiro Kameta*, *Mitsutoshi Masuda*,* *Hiroyuki Minamikawa*, *Nikolay V. Goutev*, *Jeong A. Rim*, *Jong H. Jung*, and *Toshimi Shimizu**

Hollow supramolecular nanotube architectures based on amphiphilic molecules have attracted great interest due to their potential medical and industrial encapsulation applications, as well as for filtration and purification applications.[1] Encapsulation of 1–3 nm gold nanoparticles in hollow cylinders of glycolipid nanotubes resulted in the fabrication of gold nanowires with widths regulated by the inner diameters of the nanotubes.[2] Furthermore, appropriate functionalities on the outer and inner surfaces of the nanotubes have been reported to play a significant role in the detection,[3] separation,[4] delivery,[5] and patterning[6] of biomolecules. These intriguing features and results have led us to conceive that lipid nanotubes functionalized with different outer and inner surfaces may be able to achieve the selective and effective encapsulation of biologically important polymers under ambient conditions. Lipid nanotubes with positively charged inner surfaces are of special interest for encapsulating anionic biopolymers, such as DNA, RNA, and proteins. The so-called "unsymmetrical bolaamphiphiles", 1,ω-bipolar amphiphiles in which two hydrophilic head groups of different sizes are connected to a hydrophobic spacer at each end, are promising candidates for self-assembly into nanotubes due to their asymmetry.[7] However, unsymmetrical bolaamphiphiles are known to exhibit polymorphism depending on whether the monolayer lipid membrane (MLM) is unsymmetrical or symmetrical, wherein the molecules pack in parallel and antiparallel fashions, respectively.[8–10] Most unsymmetrical bolaamphiphiles form symmetrical MLMs due to favorable antiparallel packing of the molecules.[11] The symmetrical MLMs tend to lead to flat or twisted-tape-like morphologies instead of nanotubes.[11] Although several attempts to make nanotubes have been suc-

[*] Dr. M. Masuda, Dr. T. Shimizu, Dr. N. Kameta, Dr. H. Minamikawa
Nanoarchitectonics Research Center (NARC)
National Institute of Advanced Industrial Science and Technology (AIST)
Tsukuba Central 5, 1-1-1 Higashi, Tsukuba,
Ibaraki 305-8565 (Japan)
E-Mail: m-masuda@aist.go.jp; tshmz-shimizu@aist.go.jp
Dr. M. Masuda, Dr. T. Shimizu, Dr. H. Minamikawa,
Dr. N. V. Goutev
CREST
Japan Science and Technology Agency (JST)
Tsukuba Central 4, 1-1-1 Higashi, Tsukuba, Ibaraki 305-8562 (Japan)
Dr. J. A. Rim, Dr. J. H. Jung
Nano Material Team
Korea Basic Science Institute (KBSI)
52 Yeoeun-dong, Yusung-gu, Daejeon 305-333 (Korea)

  DOI: 10.1002/adma.200501092